

DIRECTION DEPENDENT SELF CALIBRATION OF LARGE DISTRIBUTED SENSOR ARRAYS

Brian D. Jeffs[†], Sebastiaan van der Tol[‡], and Alle-Jan van der Veen[‡]

[†]Brigham Young University: bjeffs@ee.byu.edu

[‡]Delft University of Technology: S.vanderTol@ewi.tudelft.nl, allejan@cas.et.tudelft.nl.

ABSTRACT

The LOFAR astronomical array currently under development in The Netherlands will produce synthesis images of the most distant (and thus oldest) space objects by observing at unusually low frequencies (30-250 MHz) over a large aperture (100 km) using many antennas (on the order of 10,000). This presents some significant challenges for sensor calibration because at these frequencies Earth's ionosphere acts as a random refractive sheet which over the large aperture induces source direction dependent gain and phase errors that must be estimated and calibrated out. Existing array self calibration algorithms used at higher frequencies by other radio astronomy instruments such as the Very Large Array (VLA) do not address direction dependence and will not work in the LOFAR environment. A new algorithm called "demixed peeling" is presented and assessed as a solution to the direction dependent calibration problem for large distributed sensor arrays.

1. INTRODUCTION

The LOFAR radio telescope currently being developed by ATRON will operate at 20MHz-240MHz. These frequencies are lower than the operating frequencies of most radio telescopes currently in use. At lower frequencies new calibration problems arise because the effects of the ionosphere are more severe. More specifically, the calibration will be look-direction dependent and rapidly changing over time. In this paper we will describe a self calibration algorithm that was introduced in [1] called peeling. In section 3 we introduce an extension to reduce the number of iterations of the peeling algorithm

Experience with LOFAR calibration will be important for future radio telescopes like the Square Kilometer Array (SKA), which is currently being designed. The methods presented in this paper could also be relevant to similar problems outside the field of radio astronomy, such as SONAR direction finding through turbulent water.

1.1. Selfcalibration for the LOFAR Radio Telescope

The LOFAR array will be located in The Netherlands and have an overall apertures of approximately 100 km. Figure 1 illustrates a possible geometry for the planned 72 station array. Each station contains 100 dual polarization antennas covering a 100 m diameter area. Antenna signals will be combined in a digital beamformer to electronically steer a pencil beam in each station to track the deep space objects of interest. At central processor level a station can be considered as a single directional antenna. Cross correlations between signals from all stations are computed to form the basic data set for synthesis imaging. The end product is a data cube consisting of an image or intensity map of the field of view per frequency channel.

This project was supported by STW, The Netherlands

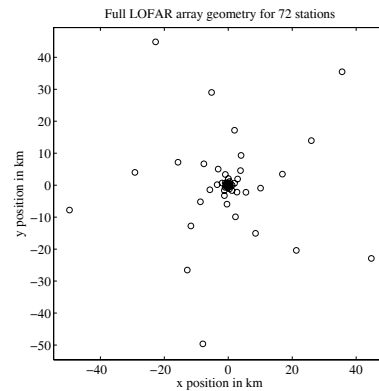


Fig. 1. Possible geometry for the full LOFAR array. Each circle represents a LOFAR station which acts as a single beamformed directional sensor element in the full array.

Radio imaging arrays use the brighter sources in the field of view as references to calibrate unknown instrumental and propagation gains and phases. This method is often referred to as "self calibration". It is assumed that the measured signal is dominated by reference sources whose position and brightness are known from previous surveys and are catalogued. LOFAR surveys will extend and improve the source catalogs, providing more reference sources for future calibration.

The ionosphere is the outer layer of the earth atmosphere. Radiation from the sun partly ionizes the atmosphere and the resulting free electrons slow down electromagnetic waves propagating through the ionosphere. This additional propagation delay is proportional to the wavelength squared, hence the corresponding phase shift is proportional to the wavelength. Therefore at lower frequencies the effects of the ionosphere are more severe. Turbulence in the ionosphere causes the electron density to fluctuate both in space and in time. These effects have a significant impact on LOFAR because of its low operational frequency. Because both the distance between the stations and the size of the beams are larger than the irregularity scale of the ionosphere LOFAR calibration is look-direction dependent. No algorithm has previously been available for direction dependent self calibration of radio imaging arrays.

2. DATA MODEL

Notation: The transpose operator is denoted by T , complex conjugate by $*$, and conjugate transpose by H . An estimated value is denoted by $\hat{\cdot}$, an expected value by $E[\cdot]$, and \odot is the element-wise

matrix multiplication (Hadamard product).

Assume that the observed signal is dominated by Q bright calibrator point sources. For narrowband observation the complex baseband signal across the array is given by

$$\begin{aligned} \mathbf{x}_k[m] &= [x_{k,1}[m], \dots, x_{k,I}[m]]^\top \\ &= \sum_{q=1}^Q \mathbf{a}_{k,q}[m] s_{k,q}[m] + \boldsymbol{\eta}_k[m] \end{aligned}$$

where $x_{k,i}[m]$ is the m^{th} time sample of the beamformed signal for station i , $1 \leq i \leq I$, in subband k centered at f_k Hz. $s_{k,q}[m]$ is the signal from the q^{th} ‘‘calibrator’’ source, $\mathbf{a}_{k,q}[m]$ is the array response vector for this source, and $\boldsymbol{\eta}_k[m]$ is the spatially and temporally white noise sample vector. Due to earth rotation the geometrical delay component of $\mathbf{a}_{k,q}[m]$ changes slowly with time, which is a critical feature exploited in synthesis imaging. Calibrator locations and intensities are accurately tabulated in star catalogues.

Assuming that $\mathbf{a}_{k,q}[m]$ is constant over M samples, called the short term integration (STI) interval, the time-frequency dependent sample autocovariance matrix for $(n-1)M \leq m \leq nM-1$ is

$$\begin{aligned} \hat{\mathbf{R}}_{k,n} &= \frac{1}{M} \sum_{m=(n-1)M}^{nM-1} \mathbf{x}_k[m] \mathbf{x}_k^H[m] \\ &\approx \mathbf{R}_{k,n} = \mathbf{A}_{k,n} \boldsymbol{\Sigma}_k \mathbf{A}_{k,n}^H + \boldsymbol{\Lambda}_k, \text{ where} \quad (1) \\ \mathbf{A}_{k,n} &= [\mathbf{a}_{k,n,1}, \dots, \mathbf{a}_{k,n,Q}]. \end{aligned}$$

$\boldsymbol{\Sigma}_k$ and $\boldsymbol{\Lambda}$ are diagonal matrices with elements $\sigma_{k,q}^2$, $1 \leq q \leq Q$ and $\lambda_{k,i}^2$ corresponding to the calibrator source powers and station noise variance respectively. In radio astronomy, elements of $\mathbf{R}_{k,n}$ are called ‘‘visibilities’’ [2]. Each visibility represents the interferometric correlation along the baseline vector between the two corresponding array elements.

$\mathbf{a}_{k,n,q}$ can be factored into the product of a known phase term $\mathbf{k}_{k,n,q}$ due entirely to propagation delay for the array and source geometry, and an unknown complex calibration gain $\mathbf{g}_{k,n,q}$ which includes both source direction dependent ionospheric perturbations and electronic instrumentation gain errors,

$$\mathbf{A}_{k,n} = \mathbf{G}_{k,n} \odot \mathbf{K}_{k,n} = [\mathbf{g}_{k,n,1} \odot \mathbf{k}_{k,n,1}, \dots, \mathbf{g}_{k,n,Q} \odot \mathbf{k}_{k,n,Q}] \quad (2)$$

Direction dependence is modeled with a distinct calibration vector, $\mathbf{g}_{k,n,q}$, for each source q .

The problem at hand is to estimate $\mathbf{G}_{k,n}$ over a range of k and n given a series of sample covariances $\hat{\mathbf{R}}_{k,n}$. Substituting (2) into (1) yields the visibility measurement equation (ME) [3]

$$\text{ME}_{k,n}(\mathbf{G}, \boldsymbol{\Lambda}) = (\mathbf{G} \odot \mathbf{K}_{k,n}) \boldsymbol{\Sigma}_k (\mathbf{K}_{k,n}^H \odot \mathbf{G}^H) + \boldsymbol{\Lambda}.$$

For a single STI the least squares calibration solution is

$$\hat{\mathbf{G}}_{k,n}, \hat{\boldsymbol{\Lambda}}_k = \arg \min_{\mathbf{G}, \boldsymbol{\Lambda}} \|\hat{\mathbf{R}}_{k,n} - \text{ME}_{k,n}(\mathbf{G}, \boldsymbol{\Lambda})\|_F^2 \quad (3)$$

where $\|\cdot\|_F$ denotes the Frobenius norm.

Direct solution of (3) is not computationally practical and we have found that for direction dependent calibration, $\mathbf{G}_{k,n}$ is not identifiable through $\hat{\mathbf{R}}_{k,n}$ unless some constraining structure over k and n exists and is exploited in the estimation algorithm. We have used

2-D polynomials in f_k and t_n to realistically model magnitude and phase as a smoothly varying function of frequency and time:

$$\begin{aligned} \mathbf{G}_{k,n}(\mathbf{p}) &= \boldsymbol{\Gamma}_{k,n}(\mathbf{p}) \odot \exp\{j\boldsymbol{\Psi}_{k,n}(\mathbf{p})\} \quad (4) \\ \boldsymbol{\Gamma}_{k,n}(\mathbf{p}) &= \sum_{d=1}^D \mathbf{Y}_d f_k^{\kappa_d} t_n^{\eta_d}, \quad \boldsymbol{\Psi}_{k,n}(\mathbf{p}) = \sum_{d=1}^D \mathbf{T}_d f_k^{\kappa_d} t_n^{\eta_d} \\ \mathbf{p} &= [\text{vec}\{\mathbf{Y}_1\}^\top, \dots, \text{vec}\{\mathbf{Y}_D\}^\top, \\ &\quad \text{vec}\{\mathbf{T}_1\}^\top, \dots, \text{vec}\{\mathbf{T}_D\}^\top, \text{diag}\{\boldsymbol{\Lambda}\}^\top]^\top. \quad (5) \end{aligned}$$

\mathbf{Y}_d and \mathbf{T}_d are the $I \times Q$ gain and phase coefficient matrices respectively where κ_d and η_d are the corresponding frequency and time integer exponent powers for the d^{th} polynomial term, and D is the total number of terms. A single source gain polynomial model, $\mathbf{g}_{k,n}(\mathbf{p}_q)$, can be defined by retaining only the q^{th} columns from both $\boldsymbol{\Gamma}_{k,n}(\mathbf{p})$ and $\boldsymbol{\Psi}_{k,n}(\mathbf{p})$ in (4). \mathbf{p}_q is formed by selecting the corresponding q^{th} columns from $\mathbf{Y}_1, \dots, \mathbf{Y}_D$ and $\mathbf{T}_1, \dots, \mathbf{T}_D$.

3. THE PEELING ALGORITHM

The current leading candidate algorithm for LOFAR calibration was introduced by Jan Noordam and has been dubbed ‘‘peeling’’ due its sequential approach of successively calibrating on one bright source at a time followed by removing (peeling) that source’s contribution from the observed sample covariances, $\mathbf{R}_{k,n}$ [1]. Peeling is based on three basic simplifying assumptions:

- Joint estimation for parameters of all Q calibrator sources can be approximated with a series of single source calibration problems, in descending order of source brightness.
- Calibration gains (magnitude and phase) vary slowly and smoothly over time and frequency. Consequently over some span of at most K frequency bins and N time bins called a cell, $\mathbf{G}_{k,n}$ is approximately constant. Cell (\tilde{k}, \tilde{n}) includes all frequency-time bins in the set $\mathcal{C}_{\tilde{k}, \tilde{n}} = \{(k, n) : \tilde{k} \leq k \leq (\tilde{k} + 1)K - 1, \tilde{n}N \leq n \leq (\tilde{n} + 1)N - 1\}$.
- Over a cell the variations in $\mathbf{K}_{k,n}$ (a.k.a. fringe rotations) due to Earth rotation and frequency change are large.

Assuming the Q sources are ordered in descending brightness, an L pass peeling algorithm is given by

1. *Initialize:* source index $q = 1$, pass index $l = 1$, and parameter vector $\hat{\mathbf{p}}_p = \mathbf{0}$ for $1 \leq p \leq Q$.
2. *Update the residuals (peel):* For all but the q^{th} source and over all (k, n) , subtract the current best estimates of their contributions from each sample covariance,

$$\hat{\mathbf{V}}_{k,n,q} = \hat{\mathbf{R}}_{k,n} - \sum_{\substack{p=1 \\ p \neq q}}^Q \text{ME}_{k,n,p}(\mathbf{p}_p), \text{ where}$$

$$\text{ME}_{k,n,p}(\mathbf{p}) = [\mathbf{g}_{k,n}(\mathbf{p}) \odot \mathbf{k}_{k,n,p}] \sigma_{k,p}^2 [\mathbf{g}_{k,n}(\mathbf{p}) \odot \mathbf{k}_{k,n,p}]^H.$$

3. *Phase center and average:* Phase rotate source q to d.c. in each $\hat{\mathbf{V}}_{k,n,q}$ and average to attenuate non-centered sources.

$$\tilde{\mathbf{V}}_{\tilde{k}, \tilde{n}, q} = \frac{1}{KN} \times \sum_{(k,n) \in \mathcal{C}_{\tilde{k}, \tilde{n}}} \text{diag}\{\mathbf{k}_{k,n,q}^*\} \hat{\mathbf{V}}_{k,n,q} \text{diag}\{\mathbf{k}_{k,n,q}\}, \quad (6)$$

4. Estimate polynomial coefficients:

$$\hat{\mathbf{p}}_q = \arg \min_{\mathbf{p}} \sum_{(\tilde{k}, \tilde{n})} \dots \left\| \mathbf{L} \odot \mathbf{W} \odot \left(\tilde{\mathbf{V}}_{\tilde{k}, \tilde{n}, q} - b_q \mathbf{g}_{\tilde{k}, \tilde{n}}(\mathbf{p}) \mathbf{g}_{\tilde{k}, \tilde{n}}^H(\mathbf{p}) \right) \right\|_F^2,$$

where \mathbf{L} is a masking matrix of ones below the diagonal and zeros elsewhere which is used to avoid fitting to diagonal terms from $\mathbf{\Lambda}$. \mathbf{W} is a weighting matrix to whiten the noise in case the noise power is not the same for all entries.

5. *Iterate:* If $q < Q$ increment q and go to 2, else if $l < L$ increment l , set $q = 1$ and go to 2, otherwise stop.

We have found that using multiple passes, e.g. with $2 \leq L \leq 5$ reduces bias in $\hat{\mathbf{p}}_q$ which arises when averaging over a cell produces insufficient attenuation of the non centered sources in step 3. Contamination in the single source fit performed in step 4 occurs because $\tilde{\mathbf{V}}_{\tilde{k}, \tilde{n}, q}$ has contributions from more than the centered source. The next section presents a more direct method of reducing this contamination bias so that the assumption that sequential single source calibration approximates joint calibration is more nearly correct.

4. DEMIXING CALIBRATOR CROSS CONTAMINATION

In step 2 of the peeling algorithm, estimates of the contribution from each source (excluding the current centering source q) are subtracted from the observed sample covariance. The residual $\tilde{\mathbf{V}}_{k, n, q}$ is intended to contain only the contribution from source q but also has noise, and due to estimation errors in $\hat{\mathbf{p}}_p$ includes a bias caused by imperfect subtraction of the other sources. In step 3 the contributions of source q are phase rotated for coherent addition while residual errors from the other sources are attenuated by incoherent averaging due to wide variation in $\mathbf{k}_{k, n, p}$, $p \neq q$, across the cell.

The purpose of steps 2 and 3 is to form a single-source approximation of the problem. Ideally $\tilde{\mathbf{V}}_{\tilde{k}, \tilde{n}, q}$ would be equal to the single source data model, $\mathbf{V}_{k, n, q}$, for sample (k, n) at the center of cell (\tilde{k}, \tilde{n}) . Assuming the gains $\mathbf{g}_{k, n, q}$ are truly constant within the cell yields

$$\tilde{\mathbf{V}}_{\tilde{k}, \tilde{n}, q} \approx \mathbf{V}_{k, n, q} = \mathbf{g}_{k, n, q} \sigma_{k, q}^2 \mathbf{g}_{k, n, q}^H, \quad \forall (k, n) \in \mathcal{C}_{\tilde{k}, \tilde{n}}.$$

During the first algorithm pass ($l = 1$) there are no available estimates for sources $q < p \leq Q$ so their contribution cannot be subtracted in step 2. Averaging in step 3 is then not sufficient to reduce bias down to the noise level and therefore multiple successive iterations are necessary. The number of iterations can be reduced if the process starts with an initial unbiased single source estimate.

In this section we develop an unbiased estimator, $\tilde{\mathbf{V}}_{\tilde{k}, \tilde{n}, q}$, so that even on the first pass $\mathbb{E}[\tilde{\mathbf{V}}_{\tilde{k}, \tilde{n}, q}] \approx \mathbf{V}_{k, n, q}$. The algorithm works on a per cell basis, so for convenience the cell indices (\tilde{k}, \tilde{n}) will be dropped.

Assume that estimates $\hat{\mathbf{p}}_p$ for $1 \leq p < q$ have previously been computed and the corresponding sources are peeled without bias in step 2. We now seek an estimate $\hat{\mathbf{p}}_q$ which is unbiased by the presence of sources $q < p \leq Q$ in $\tilde{\mathbf{R}}_{k, n}$. At this stage $\hat{\mathbf{p}}_p = \mathbf{0}$ and $\text{ME}_{k, n, p}(\mathbf{p}) = 0$ for $q < p \leq Q$ and these sources would not be peeled. The expected value of a single entry from $\tilde{\mathbf{V}}_{k, n, q}$ can then

be expressed as

$$\begin{aligned} \mathbb{E}[\hat{v}_{k, n, i, j}] &= \sum_{p=q}^Q k_{k, n, p, i} k_{k, n, p, j}^* \nu_{p, i, j}, \quad \text{for } 1 \leq i, j \leq I, \\ \nu_{p, i, j} &= \sigma_{k, p}^2 g_{p, i} g_{p, j}^* \end{aligned} \quad (7)$$

The summation in (7) can be written as an inner product

$$\mathbb{E}[\hat{v}_{k, n, i, j}] = [k_{k, n, q, i} k_{k, n, q, j}^* \quad \dots \quad k_{k, n, Q, i} k_{k, n, Q, j}^*] \boldsymbol{\nu}_{i, j}$$

where

$$\boldsymbol{\nu}_{i, j} = [\nu_{q, i, j}, \dots, \nu_{Q, i, j}]^T.$$

This gives us one equation per (k, n) pair. We can stack all these equations into a single matrix form. Let

$$\tilde{\mathbf{K}}_{i, j} = \begin{bmatrix} k_{1, 1, q, i} k_{1, 1, q, j}^* & \dots & k_{1, 1, Q, i} k_{1, 1, Q, j}^* \\ \vdots & \ddots & \vdots \\ k_{K_c, L_c, q, i} k_{K_c, L_c, q, j}^* & \dots & k_{K_c, L_c, Q, i} k_{K_c, L_c, Q, j}^* \end{bmatrix}$$

and

$$\hat{\mathbf{v}}_{i, j} = [\hat{v}_{1, 1, i, j}, \dots, \hat{v}_{K_c, L_c, i, j}]^T$$

then

$$\mathbb{E}[\hat{\mathbf{v}}_{i, j}] = \tilde{\mathbf{K}} \boldsymbol{\nu}_{i, j}.$$

Multiplying both sides with the pseudo inverse of $\tilde{\mathbf{K}}$, $\tilde{\mathbf{K}}^\dagger = (\tilde{\mathbf{K}}^H \tilde{\mathbf{K}})^{-1} \tilde{\mathbf{K}}^H$, we obtain

$$\mathbb{E}[(\tilde{\mathbf{K}}^H \tilde{\mathbf{K}})^{-1} \tilde{\mathbf{K}}^H \hat{\mathbf{v}}_{i, j}] = \boldsymbol{\nu}_{i, j}.$$

Thus

$$\hat{\mathbf{v}}_{i, j} = (\tilde{\mathbf{K}}^H \tilde{\mathbf{K}})^{-1} \tilde{\mathbf{K}}^H \hat{\mathbf{v}}_{i, j} \quad (8)$$

is the least squares estimator we are looking for.

A closer look at (8) reveals that it is directly related to the original approach of phase centering and averaging. First define

$$\mathbf{C} = KN(\tilde{\mathbf{K}}^H \tilde{\mathbf{K}})^{-1}$$

Now we can write

$$\hat{\mathbf{v}}_{i, j} = \mathbf{C} \frac{1}{KN} \tilde{\mathbf{K}}^H \hat{\mathbf{v}}_{i, j} = \mathbf{C} \tilde{\mathbf{v}}_{i, j}$$

where $\tilde{\mathbf{v}}_{i, j} = \frac{1}{KN} \tilde{\mathbf{K}}^H \hat{\mathbf{v}}_{i, j}$. Comparison of the structure of this matrix equation with the summation operation of (6) reveals that the first element of $\tilde{\mathbf{v}}_{i, j}$ is equal to the $(i, j)^{\text{th}}$ element of $\tilde{\mathbf{V}}_{\tilde{k}, \tilde{n}, q}$. The remaining elements of $\tilde{\mathbf{v}}_{i, j}$ correspond to evaluating (6) for sources $q + 1$ to Q . Thus computing $\tilde{\mathbf{v}}_{i, j} = \frac{1}{KN} \tilde{\mathbf{K}}^H \hat{\mathbf{v}}_{i, j}$ performs an element-wise version of the peeling phase centering and averaging step on not just q , but for all sources q to Q . The multiplication by inversion matrix \mathbf{C} 'demixes' the contributions of the sources into separate single source problems.

The estimates $\hat{\mathbf{p}}_p$ are based on all samples in the domain. The demixing algorithm works only on a single cell. Therefore the result of removing a contaminating source by demixing is noisier than removing a source by conventional peeling subtraction.

The noise amplification by demixing depends on the condition of \mathbf{C} . Because of the third assumption of Section 3, large fringe rotations within a cell, \mathbf{C} will be well conditioned. For large cells, \mathbf{C} will converge to the identity matrix.

The optimal weight for a least squares fit is known to be the inverse of the asymptotic covariance of the residuals [4]. For low SNR the cross correlation of the residuals is small. The optimal weighting

Source	Catalog Name	RA ^o	DEC ^o	SNR dB
1	3C461	350.8	58.8	-20.7
2	3C405	299.9	40.7	-21.0
3	3C86	51.8	55.3	-30.0

Table 1. Three brightest calibrator sources

is then given by the inverse of the variances. This weighting can be achieved by setting the entries of \mathbf{W} in step 4 to

$$w_{i,j} = 1/\text{stddev}(\hat{\nu}_{i,j,1}) = \left(\frac{\sigma^2 c_{1,1}}{KN} \right)^{-1/2}$$

where $c_{1,1}$ is the top left entry of \mathbf{C} , σ^2 is the variance of the entries of $\hat{\mathbf{V}}$. An estimate of σ^2 is the product of the diagonal entries of $\hat{\mathbf{V}}$, $\hat{\sigma}^2 = \hat{\nu}_{i,i} \hat{\nu}_{j,j}$.

5. SIMULATION RESULTS

Performance of the peeling algorithm and demixing procedure were evaluated by computer simulation. A realistic self calibration scenario was modeled using the LOFAR geometry of Figure 1, but with every other station deleted to form a 36 element array for reduced computational complexity. Station beams were pointed at right ascension (RA) 54.0^o and declination (DEC) 55.1^o.¹ An accurate model based on the existing LOFAR initial test station (ITS) [5] was used for the station beam directional response, including sidelobe fine structure. For this 40 MHz observation, the -3 dB beamwidth was approximately 5^o with sidelobe peak levels typically -13 dB below the mainlobe.

The $Q = 3$ brightest radio sources after beamforming were included in the simulation. Table 1 lists their locations, taken from the standard 3C and 4C radio survey catalogues, and apparent SNRs computed from tabulated flux values assuming sky noise limited reception. Source 3 is seen within the station beam mainlobe while 1 and 2 appear in deep sidelobes.

A first order 2-D polynomial was applied both for synthesizing array data, $\mathbf{x}_k[m]$, and in the peeling algorithm parameter model. Cells consisted of $K = 50$ frequency bins covering 100 kHz, and $L = 10$ time bins. Ten cells, $1 \leq k \leq 10$, $\tilde{n} = 1$, were used to fit a first order (d.c. and slope term) polynomial in frequency, so $\mathbf{\Gamma}_{k,n}(\mathbf{p}) = \mathbf{Y}_1 + \mathbf{Y}_2 f_k$ and $\mathbf{\Psi}_{k,n}(\mathbf{p}) = \mathbf{T}_1 + \mathbf{T}_2 f_k$. The “true” parameter matrices were randomly generated.

Figure 2 presents results of Monte Carlo trial simulations to evaluate peeling squared bias error in with and without the demixing procedure. Error was computed by comparing estimated polynomial coefficients from $\hat{\mathbf{p}}_q$, $1 \leq q \leq Q = 3$ with the true \mathbf{Y}_d and \mathbf{T}_d .

Estimation error variance (not shown) was acceptably low and the same level with and without demixing. But as can be seen, demixing significantly reduced bias error which we believe is due to contamination from the other sources when applying the single source model in peeling step 3. Averaging across all parameters for each source yields an average bias reduction by a factor of 17.7 for source 1, 3.33 for source 2, and 3.71 for source 3.

Without demixing, peeling requires $I = 3$ passes to reduce bias levels to compare with one pass of demixed peeling. However,

¹RA and DEC are astronomical polar coordinates for fixed locations in the celestial sphere used to locate deep space objects; the celestial equivalent of latitude and longitude. See e.g. <http://liftoff.msfc.nasa.gov/academy/universe/radec.html>.

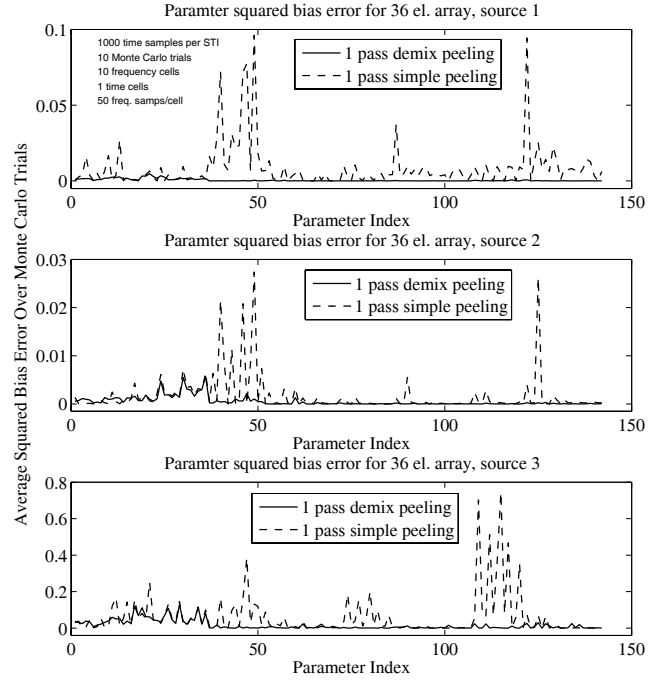


Fig. 2. Comparison of bias error in estimating polynomial parameter \mathbf{p}_q , $1 \leq q \leq 3$ for peeling alone, and peeling with demixing. One peeling pass was performed in each case. The parameter index number is a function of station index, i and polynomial term index, d , and is ordered as in (5) and text following.

though this demonstrates the theoretical correctness of the approach described in Section 4, its practical utility is questionable. With our simulation implementation in MATLAB it takes 3.31 times as long to complete a single demix pass as does a three pass regular peeling algorithm to produce similar quality parameter estimates. We are currently investigating methods to code demixing more efficiently, but for the present time we believe that the multi-pass peeling algorithm of Section 3 is the best candidate for direction dependent calibration of the LOFAR radio astronomy array.

6. REFERENCES

- [1] J. E. Noordam, “LOFAR calibration challenges,” in *Proceedings of the SPIE, Vol. 5489, pp. 817-825 (2004)*, Oct. 2004, pp. 817–825.
- [2] A. Thompson, J. Moran, and G. Swenson Jr., *Interferometry and Synthesis in Radio Astronomy, Second Edition*. New York: Wiley-Interscience, 2001.
- [3] J. Noordam, “The measurement equation of a generic radio telescope, aips++ implementation note nr 185,” ASTRON, Tech. Rep., 1996.
- [4] B. Ottersten, P. Stoica, and R. Roy, “Covariance matching estimation techniques for array signal processing applications,” *Digital Signal Processing Rev. J.*, vol. 8, pp. 185–210, 1998.
- [5] S. Wijnholds, J. Bregman, and A. Boonstra, “Sky noise limited snapshot imaging in the presence of rfi with lofar’s initial test station,” to appear in *Experimental Astronomy*, 2005.